2016 12th World Congress on Intelligent Control and Automation (WCICA)
June 12-15, 2016, Guilin, China

Optimization Algorithm of Serial Manipulator Structure Based on Posture Manipulability

Shiyuan Jia, Yinghong Jia, and Shijie Xu

***Abstract*— To solve the optimization problem of manipulator, the concept of posture manipulability is proposed based on the numerical method of posture dexterity. On the basis of posture dexterity and manipulability, an algorithm on structure optimization design to manipulator is proposed. Based on the original structure design, this method, taking the reciprocal of posture-manipulability as fitness function, optimizes manipulator structural parameters to maximize the operability by using genetic algorithm. Posture-manipulability was deduced in detail for a six-degree of freedom (DOF) manipulator. Under the condition of self-collision, optimization algorithm is used to optimize length parameters, which increased posture manipulability by 40.33%. Finally, arm dexterous workspace is presented before and after optimization, and validity of the algorithm is tested. Results show that manipulators, designed by structural optimization method, have high operability.**

I. Introduction

Several criteria have been used in the past for the design of robotic manipulators. Many scholars, such as Gupta, Roth and Lee have analyzed the workspace of manipulators and have sometimes used it as a design criterion. Two issues of reference [1] are discussed: Given the structure, what is the workspace? Alternatively, given a desired workspace, what should the manipulator's structure be? Paulo[2] proposed a method of calculation of the workspace boundary and took the workspace volume as objective function to optimize a 3R manipulator. Snyman[3] proposed a numerical optimization algorithm to determine the boundaries of the workspaces of planar manipulators. On the basis of the workspace, other scholars have investigated the possibility of defining dexterity or manipulability. Gosselin[4] takes condition number of Jacobian matrix as a key consideration for manipulator design. As a design criterion, condition number satisfies the requirement of kinematics invertibility as well as provides a basis for the optimization of path planning of robot arm, but it is not suitable for a global performance index for manipulator design. By combining the condition number and workspace, Gosselin[5] puts forward the global condition index (global conditioning index, GCI), GCI is a kind of performance index based on the distribution of condition number in the whole workspace. Reference [6] takes isotropic condition number as the objective function, optimize structure parameters to maximize its kinematics performance; Reference [7, 8] use local condition index or global condition index to optimize different manipulator configuration; Reference [9] illustrates the deficiency of traditional performance index such as Jacobi matrix condition number, manipulability and GCI. In addition, a task-oriented manipulability measure is proposed by reference [10].

With the improvement of task demands for industrial robot and space robot, to meet multitask and versatility of robot arm, the manipulator dexterity and manipulability are particularly important. Based on the above design index, this paper presents the numerical method of posture dexterity and posture-manipulability algorithm by bringing in the concept of "working sphere". A structure optimization method for manipulator is proposed based on the posture-manipulability. The algorithm can realize global optimization to robot arm.

The posture dexterity of each end-effector point is solved by inverse kinematics algorithm for a 6R manipulator. The dexterity reflects the possible orientations associated with each end-effector point. The posture-manipulability can be obtained on the foundation of dexterity. Taken the reciprocal of posture-manipulability as fitness function, genetic algorithm is used to optimize the manipulator structure parameters. Arm dexterous workspace is drawn before and after optimization. The results show that manipulators, acquired by optimization algorithm, have good operability.

II. The Definition of Posture Dexterity and Posture Manipulability

The manipulator posture dexterity can be measured by pose probability coefficient. According to Fig. 1, R_1, R_2, R_3 are the first three revolute joints, and the latter three joints can be seen as a spherical hinge with its center on wrist point P_w. At this point, the concept of "working sphere" is introduced. Cartesian coordinate system $S-Oxyz$ is established in workspace, and $P_1(x_1, y_1, z_1)$ is a working point in workspace. A sphere, taking working point as its center and end link (or end-effector) as its radius, is called "working sphere". Ideally, the wrist point P_w can reach arbitrary point of the sphere, and the end link can reach working point passing through the wrist point. But in fact, because of the structure constraint, the wrist point can only reach part area of the sphere. The larger the area is, the better the posture dexterity is. Posture dexterity is defined by numerical discrete points on the spherical surface, which can be measured by pose probability coefficient φ. The existence of joint solutions corresponding to N points sampled

This work was supported by National Natural Science Foundation of China under Grant 11272027.

Shiyuan Jia is with School of Astronautics, Beihang University, Beijing 100191, China (phone: 01082339751; e-mail: jiashi.yuan@ 163.com).

Yinghong Jia is with School of Astronautics, Beihang University, Beijing 100191, China (e-mail: jia_yingh@163.com).

Shijie Xu is with School of Astronautics, Beihang University, Beijing 100191, China.

uniformly on working sphere surface is analyzed. The number of wrist points, making end point arrive at working point through sample point, is n. Therefore, the pose probability coefficient is

$$\varphi = n/N \quad \varphi \le 1. \tag{1}$$

$\varphi=1$ means that any orientation of working point results in a feasible arm pose.

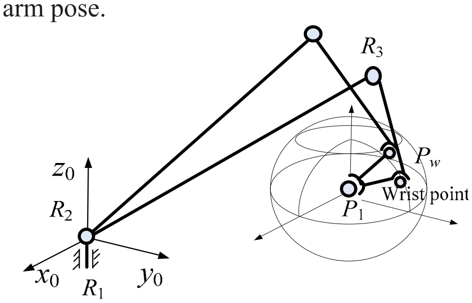

Fig. 1. Manipulator end-effector "working sphere"

The forward kinematics is proposed as follows:

$$^{0}\boldsymbol{T}_n = {}^{0}\boldsymbol{T}_1 {}^{1}\boldsymbol{T}_2 \cdots {}^{n-1}\boldsymbol{T}_n \tag{2}$$

where $^{i-1}\boldsymbol{T}_i$ is coordinate-transformation matrix from coordinate S_i to coordinate S_{i-1}; If $^{0}\boldsymbol{T}_n$ is known, joint solutions can be solved by inverse kinematics. The general recursive procedure is as follows:

$$\left.\begin{aligned} &[{}^{0}\boldsymbol{T}_1]^{-1}\,{}^{0}\boldsymbol{T}_n = {}^{1}\boldsymbol{T}_2 \cdots {}^{n-1}\boldsymbol{T}_n \Rightarrow q_1 \\ &[{}^{1}\boldsymbol{T}_2]^{-1}[{}^{0}\boldsymbol{T}_1]^{-1}\,{}^{0}\boldsymbol{T}_n = {}^{2}\boldsymbol{T}_3 \cdots {}^{n-1}\boldsymbol{T}_n \Rightarrow q_2 \\ &\vdots \\ &[{}^{n-2}\boldsymbol{T}_{n-1}]^{-1} \cdots [{}^{1}\boldsymbol{T}_2]^{-1}[{}^{0}\boldsymbol{T}_1]^{-1}\,{}^{0}\boldsymbol{T}_n = {}^{n-1}\boldsymbol{T}_n \Rightarrow q_n \end{aligned}\right\} \tag{3}$$

where $\boldsymbol{q} = (q_1, q_2, \cdots, q_n)^T$ denote joint variables vector.

The above-defined pose probability coefficient of dexterity can determine the dexterity of working point, but it cannot judge the overall performance of the whole workspace. The posture-manipulability is defined based on the dexterity, which is the percentage of sampled working points whose pose probability coefficient is bigger than a given value. The calculation method of posture-manipulability is as follows:

$$\lambda(\alpha) = [\sum_{i=1}^{M} (\varphi_i > \alpha)] / M \tag{4}$$

where φ_i --the pose probability coefficient of ith sampled working point; M--the number of sampled working points in workspace; α --given value of pose probability coefficient.

III. Kinematic performance indices based on the Jacobian matrix

A. Jacobian matrix

Considering a robot arm with n DOF, the generalized input velocity vector is $\dot{\boldsymbol{q}} = (\dot{q}_1, \dot{q}_2, \cdots, \dot{q}_n)^T$, and the generalized output velocity vector $\boldsymbol{V} = (v, \omega)^T$ represents the translation and rotation velocities of the end-effector. The output velocity $\boldsymbol{V}$ is related to the input velocity $\dot{\boldsymbol{q}}$ by

$$\boldsymbol{V} = \boldsymbol{J}\dot{\boldsymbol{q}} \tag{5}$$

where the linear operator $\boldsymbol{J}$ is the Jacobian matrix, and the Jacobian matrix reflects the linear mapping from the joint space to the Cartesian space. The inverse relation can be derived by introducing the generalized inverse matrix of $\boldsymbol{J}$ (i.e., the Moore-Penrose pseudoinverse $\boldsymbol{J}^{+}$ [11]).

$$\dot{\boldsymbol{q}} = \boldsymbol{J}^{+}\boldsymbol{V} \tag{6}$$

By screw theory[12]-[13], Jacobian matrix can be solved as follows:

$$\boldsymbol{J} = (\xi_1' \quad \xi_2' \quad \cdots \quad \xi_n') \tag{7}$$

where ξ_i' is the ith motion screw of joint, which can be calculated by:

$$\xi_i' = \begin{bmatrix} \boldsymbol{\omega}_i' \\ \boldsymbol{r}_i' \times \boldsymbol{\omega}_i' \end{bmatrix} \tag{8}$$

where $\boldsymbol{r}_i'$ is the position vector of one point on joint axis under the current configuration, and $\boldsymbol{\omega}_i'$ is the unit vector of joint axis under the current configuration, who meet

$$\boldsymbol{\omega}_i' = e^{q_1\hat{\omega}_1} e^{q_2\hat{\omega}_2} \cdots e^{q_{i-1}\hat{\omega}_{i-1}} \boldsymbol{\omega}_i \tag{9}$$

$$\begin{bmatrix} \boldsymbol{r}_i' \\ 1 \end{bmatrix} = e^{q_1\hat{\xi}_1} e^{q_2\hat{\xi}_2} \cdots e^{q_{i-1}\hat{\xi}_{i-1}} \begin{bmatrix} \boldsymbol{r}_i(0) \\ 1 \end{bmatrix} \tag{10}$$

where $\boldsymbol{\omega}_i$ is the unit vector of joint axis under the initial configuration, $\boldsymbol{r}_i(0)$ is the position vector of one point in joint axis under the initial configuration.

B. Manipulability ellipsoid

For any matrix $\boldsymbol{J} \in \boldsymbol{R}^{m\times n}$, there exist unitary matrices $\boldsymbol{U} \in \boldsymbol{R}^{m\times m}$ and $\boldsymbol{V} \in \boldsymbol{R}^{n\times n}$ such that

$$\boldsymbol{J} = \boldsymbol{U\Sigma V}^T \tag{11}$$

where

$$\boldsymbol{\Sigma} = \begin{bmatrix} \sigma_1 & & & 0 & \\ & \sigma_2 & & & \\ & & \ddots & & \boldsymbol{0} \\ 0 & & & \sigma_m & \end{bmatrix} \in \boldsymbol{R}^{m\times n} \tag{12}$$

with

$$\sigma_1 \ge \sigma_2 \ge \cdots \ge \sigma_m \ge 0 \tag{13}$$

In order to compare manipulators of different sizes and configurations fairly and reveal the transmission efficiency from the joint space to the Cartesian space intuitively, normalization is performed on input velocity vector $\dot{\boldsymbol{q}}$ as follows; therefore, the joint space becomes a unit sphere, as in Fig.2

$$\|\dot{\boldsymbol{q}}\| \le 1 \tag{14}$$

which leads to

$$\boldsymbol{V}^T (\boldsymbol{JJ}^T)^{+} \boldsymbol{V} \le 1 \tag{15}$$

If the Euclidean norm is used, then (14) represents a circle in the joint space. This circle is mapped through matrix $(\boldsymbol{JJ}^T)^{+}$ into an ellipse, usually called the *manipulability ellipsoid*[14]-[15], in the generalized coordinates' space as in Fig. 2.

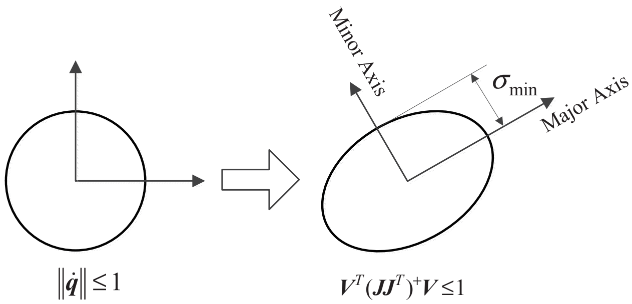

Fig. 2. The manipulability ellipsoid

The velocity minimum of the ellipsoid is the minimum singular value of the linear operator $\boldsymbol{J}$, which means the kinematic transmission ability in the direction of the robot's worst speed performance, with better kinematic transmission ability for a bigger minimum singular value.

$$\sigma_{\min} = \min(\sigma_i) \rightarrow \max \tag{16}$$

where σ_i is the singular value of $\boldsymbol{J}$. The robot is in a singularity type, when at least one singular value is zero, and the robot is close to a singularity type, when $\sigma_{\min}$ is close to zero. Consequently, the joint velocity will be infinite for some output velocity; therefore, the minimum singular value of the Jacobian matrix should be large enough to control the robot.

C. Condition number

A large dimension along a given axis of the manipulability ellipsoid indicates a large amplification error. It is therefore necessary to quantify this amplification factor. Let us consider the linear system

$$\boldsymbol{J}^{+} \triangle \dot{\boldsymbol{X}} = \triangle \dot{\boldsymbol{q}} \tag{17}$$

A possible error amplification factor for this system expresses how a *relative* error in $\triangle \dot{\boldsymbol{q}}$ gets multiplied and leads to a *relative* error in $\triangle \dot{\boldsymbol{X}}$. It characterizes in some sense the dexterity of the robot and has been proposed as a performance index. We use a norm such that

$$\left\| \boldsymbol{J}^{+} \triangle \dot{\boldsymbol{X}} \right\| \leq \left\| \boldsymbol{J}^{+} \right\| \left\| \triangle \dot{\boldsymbol{X}} \right\| \tag{18}$$

and obtain

$$\frac{\left\| \triangle \dot{\boldsymbol{X}} \right\|}{\left\| \dot{\boldsymbol{X}} \right\|} \leq \left\| \boldsymbol{J}^{+} \right\| \left\| \boldsymbol{J} \right\| \frac{\left\| \triangle \dot{\boldsymbol{q}} \right\|}{\left\| \dot{\boldsymbol{q}} \right\|} \tag{19}$$

The error amplification factor, called the *condition number* κ, is therefore defined as

$$\kappa = \left\| \boldsymbol{J}^{+} \right\| \left\| \boldsymbol{J} \right\| = \sigma_{\max} / \sigma_{\min} \tag{20}$$

where $1 \leq \kappa < +\infty$, and reflects the transmission accuracy and error sensitivity. Usually the reciprocal of κ is used as the kinematic transmission accuracy index,

$$\kappa_J = \frac{1}{\left\| \boldsymbol{J}^{+} \right\| \left\| \boldsymbol{J} \right\|} = \sigma_{\min} / \sigma_{\max} \tag{21}$$

where $0 \leq \kappa_J \leq 1$. The inverse of the condition number is termed as local condition index (LCI).

IV. GENETIC ALGORITHM OF MANIPULATOR STRUCTURE OPTIMIZATION BASED ON POSTURE-MANIPULABILITY

Turn manipulator structure optimization into problem of solving minimum of evaluation function, and the performance index is the reciprocal of posture-manipulability as follows:

$$\left.\begin{aligned} &\min J(h) = 1/\lambda(\alpha) \\ &st.\ l_1 + \cdots + l_i = c \\ &\quad l_i \in [l_{i\min}, l_{i\max}] \end{aligned}\right\} \tag{22}$$

where c is the sum of the lengths of design parameters, and $[l_{i\min}, l_{i\max}]$ is the range of parameter l_i.

The flow chart of optimization algorithm is shown in Fig. 3. The optimization algorithm includes the following parts:

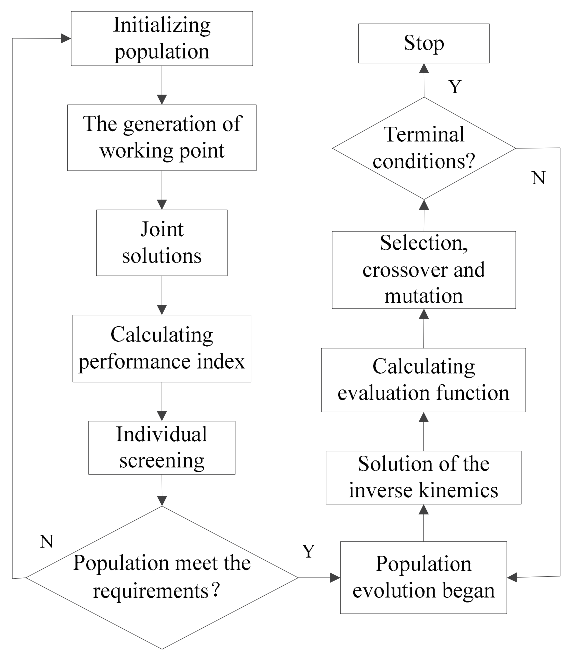

Fig. 3. The flow chart of optimization algorithm

1) Initializing population. Set the evolution generation counter $i \leftarrow 0$; Set the maximal evolution generation I; Generate K individuals as initial population P(0), where I and K is constant, and the initial structure parameter is an individual in the initial population.

2) The generation of working point and posture of end-effector. M working points are randomly generated in workspace. Working sphere is generated on each working point, and N random points are chosen on working sphere surface. The posture of end-effector is a vector, which is from random point on working sphere to working point.

3) Joint solutions are solved by inverse kinematics for any posture of each working point.

4) Calculating performance index. Pose probability coefficient of each working point is solved by inverse kinematics. By counting the pose probability coefficient, posture-manipulability can be obtained. Then, evaluation function, the reciprocal of posture-manipulability, is calculated for each individual of the population

5) Population evolution. According to the evaluation function, individuals are evaluated, and then selection, crossover and mutation operation are applied to the population.

6) Judgement of terminal conditions. If $i \le I$, then $i \leftarrow i+1$; If $i \ge I$ or $i < I$, but meeting the termination conditions, algorithm will stop and output the final solutions.

V. EXAMPLE OF 6R MANIPULATOR

A. The fitness function

Coordinate frame of 6R manipulator is shown in Fig 4:

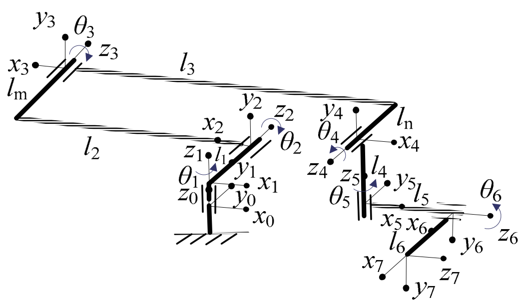

Fig.4. A 6R manipulator

According to forward kinematics of manipulator, equation (23) can be obtained:

$$ {}^{0}\boldsymbol{T}_7 = {}^{0}\boldsymbol{T}_1\,{}^{1}\boldsymbol{T}_2\,{}^{2}\boldsymbol{T}_3\,{}^{3}\boldsymbol{T}_4\,{}^{4}\boldsymbol{T}_5\,{}^{5}\boldsymbol{T}_6\,{}^{6}\boldsymbol{T}_7 = \begin{bmatrix} n_x & o_x & a_x & p_x \\ n_y & o_y & a_y & p_y \\ n_z & o_z & a_z & p_z \\ 0 & 0 & 0 & 1 \end{bmatrix} \tag{23}$$

where $\boldsymbol{n} = [n_x, n_y, n_z]^T$ is normal vector, $\boldsymbol{o} = [o_x, o_y, o_z]^T$ is direction vector, and $\boldsymbol{a} = [a_x, a_y, a_z]^T$ is approach vector. The three vectors can describe the posture of end-effector. Matrix ${}^{0}\boldsymbol{R}_7 = [\boldsymbol{n,o,a}]$ is the rotational transformation matrix from S_7 to S_0, and $\boldsymbol{p} = [p_x, p_y, p_z]^T$ is the position vector of origin of coordinate S_7 in coordinate S_0

If transformation matrix ${}^{0}\boldsymbol{T}_7$ is known, the joint solutions can be solved by equation (3), shown as follows:

$$\theta_1 = a\tan 2(\frac{k_1}{k_2}) \pm a\tan 2(\frac{\sqrt{k_1^2 + k_2^2 + k_3^2}}{k_3}) \tag{24}$$

where $k_1 = l_5 a_x + l_6 n_x - p_x$, $k_2 = -l_5 a_y - l_6 n_y + p_y$, $k_3 = l_1$

$$\theta_2 = a\tan 2(\frac{c_5 B}{c_5 A}) \pm \\ a\tan 2(\frac{\sqrt{(2l_2 c_5 B)^2 + (2l_2 c_5 A)^2 - (l_3^2 c_5^2 - l_2^2 c_5^2 - A^2 - B^2)^2}}{l_3^2 c_5^2 - l_2^2 c_5^2 - A^2 - B^2}) \tag{25}$$

$$\theta_3 = \begin{cases} \text{atan2}(\dfrac{-As_2 + Bc_2}{l_2 c_5 + Ac_2 + Bs_2}), & c_5 > 0 \\ \pi + \text{atan2}(\dfrac{-As_2 + Bc_2}{l_2 c_5 + Ac_2 + Bs_2}), & c_5 > 0 \end{cases} \tag{26}$$

where

$$A = l_4 a_z - c_5(-p_x c_1 - p_y s_1 + l_6 n_x c_1 + l_6 n_y s_1 + l_5 a_x c_1 + l_5 a_y s_1) \tag{27}$$

$$B = (l_4(a_x c_1 + l_4 a_y s_1)) - c_5(p_z - l_6 n_z - l_5 a_z) \tag{28}$$

$$\theta_4 = \theta_{234} - \theta_2 - \theta_3 \tag{29}$$

where

$$\theta_{234} = \begin{cases} a\tan 2(\dfrac{-a_z}{a_x c_1 + a_y s_1}), & c_5 > 0 \\ a\tan 2(\dfrac{a_z}{-a_x c_1 - a_y s_1}) = \pi + a\tan 2(\dfrac{-a_z}{a_x c_1 + a_y s_1}), & c_5 < 0 \end{cases} \tag{30}$$

$$\theta_5 = a\tan 2(\frac{\dfrac{l_1 + l_6(-n_x s_1 + n_y c_1) + p_x s_1 - p_y c_1}{l_5}}{(-n_x s_1 + n_y c_1)c_6 - (-o_x s_1 + o_y c_1)s_6}) \tag{31}$$

$$\theta_6 = \begin{cases} a\tan 2(\dfrac{o_x s_1 - o_y c_1}{-n_x s_1 + n_y c_1}), & c_5 > 0 \\ a\tan 2(\dfrac{-o_x s_1 + o_y c_1}{n_x s_1 - n_y c_1}) = \pi + a\tan 2(\dfrac{o_x s_1 - o_y c_1}{-n_x s_1 + n_y c_1}), & c_5 < 0 \end{cases} \tag{32}$$

The existence of joint solutions is analyzed by inverse kinematics, when the orientations associated with each end-effector point are given. The pose probability coefficient can be solved of each working point, and then the posture-manipulability of robot arm can be calculated. Finally, the evaluation function (or fitness function) can be acquired.

B. Jacobian matrix

The unit vectors of the joint axis under initial configuration in the link's reference form are

$$\begin{aligned} &\boldsymbol{\omega}_1 = \begin{bmatrix} 0 \\ 0 \\ 1 \end{bmatrix}, \boldsymbol{\omega}_2 = \begin{bmatrix} 0 \\ 1 \\ 0 \end{bmatrix}, \boldsymbol{\omega}_3 = \begin{bmatrix} 0 \\ 1 \\ 0 \end{bmatrix}, \\ &\boldsymbol{\omega}_4 = \begin{bmatrix} 0 \\ -1 \\ 0 \end{bmatrix}, \boldsymbol{\omega}_5 = \begin{bmatrix} 0 \\ 0 \\ 1 \end{bmatrix}, \boldsymbol{\omega}_6 = \begin{bmatrix} 1 \\ 0 \\ 0 \end{bmatrix} \end{aligned} \tag{33}$$

$$\begin{aligned} &\boldsymbol{r}_1 = \begin{bmatrix} 0 \\ 0 \\ 0 \end{bmatrix}, \boldsymbol{r}_2 = \begin{bmatrix} 0 \\ 0 \\ 0 \end{bmatrix}, \boldsymbol{r}_3 = \begin{bmatrix} -l_2 \\ 0 \\ 0 \end{bmatrix}, \\ &\boldsymbol{r}_4 = \begin{bmatrix} l_3 - l_2 \\ 0 \\ 0 \end{bmatrix}, \boldsymbol{r}_5 = \begin{bmatrix} l_3 - l_2 \\ l_1 \\ 0 \end{bmatrix}, \boldsymbol{r}_6 = \begin{bmatrix} l_3 - l_2 \\ l_1 \\ -l_4 \end{bmatrix} \end{aligned} \tag{34}$$

According to equation (7)-(10), the Jocabian matrix can be obtained.

C. The optimal mechanical design

To keep the original structure design, link parameters are chosen as design variables without any change in the layout of degrees of freedom. The design variables are given by:

$$h = (l_1, l_2, l_3, l_4, l_5, l_6) \tag{35}$$

where l_1, l_2, l_3, l_4, l_5 and l_6 are design variables as shown in Fig 3. The bounds are $l_1 \in [0, 0.5]$, $l_2 \in [0, 1.0]$, $l_3 \in [0, 1.0]$, $l_4 \in [0, 0.5]$, $l_5 \in [0, 0.5]$, $l_6 \in [0, 0.5]$. The initial value of design variables is $h_0 = (0.12, 0.4, 0.9, 0.1, 0.1, 0.15)$. The population size is 20, and the maximal evolution generation is 100. Crossover probability is 0.8, and mutation probability is 0.2. The terminal condition is that the average change in the fitness function is less than 10^{-4}, and the fitness function is as follows:

$$\left.\begin{aligned} &\min J(h) = 1/\lambda(\alpha) \\ &l_1 + l_2 + l_3 + l_4 + l_5 + l_6 = 1.77 \\ &h_L > 2r_L \end{aligned}\right\} \tag{36}$$

where h_L is the minimum safe distance between any pair of links, in order to prevent link interferences and r_L is the radius of the links of the robot.

VI. Results

The optimal fitness function is shown in Figs. 5. The actual evolution iteration is 61. The optimized parameters are $h' = (0.012, 0.749, 0.768, 0.149, 0.033, 0.059)$, and the posture-manipulability before and after optimization is as follows:

$$\begin{cases} \lambda(0.75) = 0.5067 \\ \lambda'(0.75) = 0.9100 \end{cases} \tag{37}$$

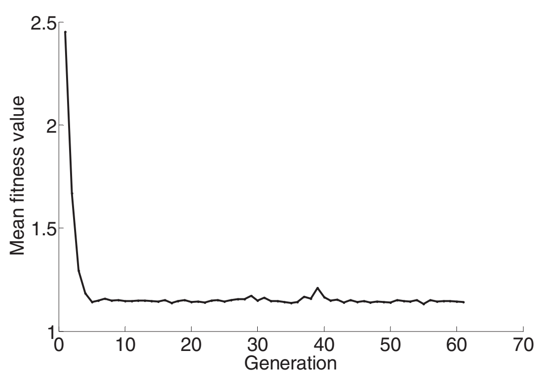

Fig. 5 Curve of fitness function

The results show that optimized link l_1 gets shorter and the optimized length is close to zero. l_2 and both become longer, while l_3, l_5 and l_6 all become shorter. The optimized length of l_2 and l_3 are basically the same. The whole manipulator can be seen as the combination of two long arms and several short arms. The configuration of manipulator is similar to human's arm. Dexterous workspace is shown in Figs. 6-7 before and after optimization. The working points successfully satisfying the dexterity criteria defined above are green colored whereas the other points are color coded from yellow to red with decreasing percentage of dexterity. The red areas mean that the pose probability coefficient of working points is smaller than 0.5. The green areas represent that the pose probability coefficient of working points is bigger than 0.75 and the yellow areas indicate the workspace with its pose probability coefficient between 0.5 and 0.75. Fig. 6 shows that the red areas are big in the edge and interior of the workspace. The above part of the manipulator has large yellow areas. After optimization the green areas increase, which means that the posture dexterity of manipulator becomes better. The LCI has increased after optimization by comparing Fig.8 to Fig.9. Setting the velocity minimum as 0.2 and the LCI minimum as 0.12, the projection drawings of LCI's distribution are shown in Fig.10-Fig.11.

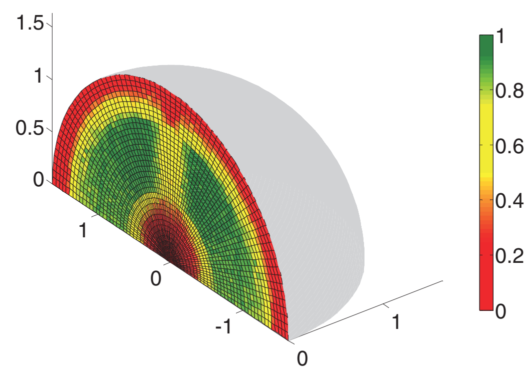

Fig.6 Dexterous workspace of manipulator before optimization

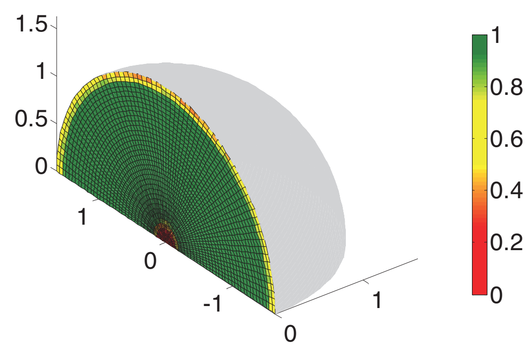

Fig.7 Dexterous workspace of manipulator after optimization

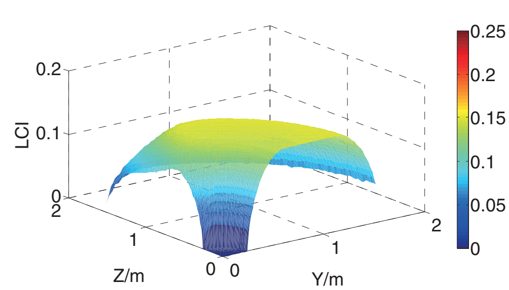

Fig. 8 LCI's distribution in workspace before optimization

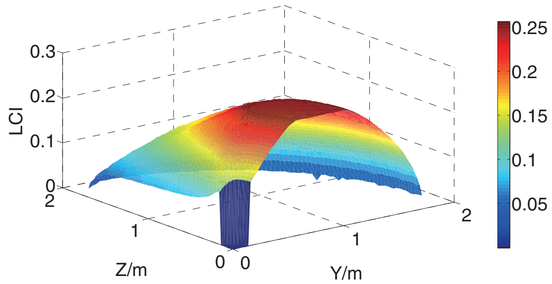

Fig. 9 LCI's distribution in workspace after optimization

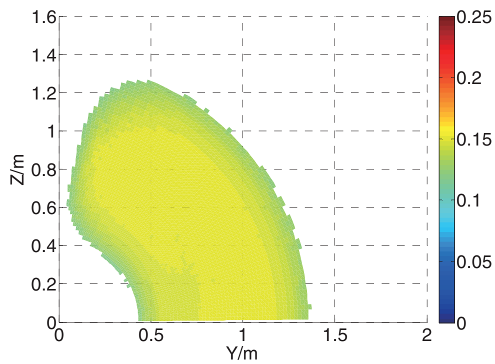

Fig.10 projection drawings of LCI's distribution before optimization

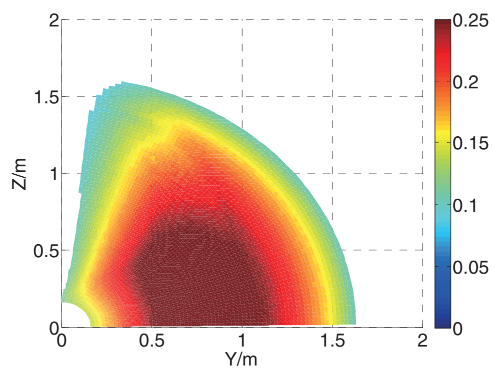

Fig. 11 projection drawings of LCI's distribution after optimization

VII. Conclusions

This paper presents a numerical calculation method of posture dexterity. Based on the numerical method of posture dexterity, a new concept of manipulability is proposed; Taken the reciprocal of posture-manipulability as fitness function, optimization structure method is proposed to maximize the operability based on genetic algorithm, which can achieve good posture-manipulability for robot arm. The results show that optimized manipulator, which is similar to human's arm, can be seen as the combination of two long arms and several short arms, and the two long arms are basically the same. In addition, the shorter the length of end-effector is, the better the posture-manipulability is. Therefore, short arms should be designed as short as they can, even can be designed as zero links. The dexterity-manipulator increased by 40.33% after optimization which means that the optimization algorithm is effective and reasonable. The transmission performance of mechanism also increased after optimization. The algorithm can also join different constraint conditions to optimize the structure of manipulator. It can also realize the design procedure: design – optimization – redesign – re-optimization to obtain a better layout of degree of freedom.

References

[1] Gupta K C, Roth B. Design Considerations for Manipulator Workspace. ASME Journal of mechanisms, Transmission, and Automation in Design, 1982, 104(1): 704-711.

[2] Bergamaschi P R, Nogueira A C, Saramago S F P. Design and optimization of 3R manipulators using the workspace features. Applied Mathematics and Computation, 172(2006) 439–463.

[3] Snyman J A, Plessis L J du, Duffy J. An Optimization Approach to the Determination of the Boundaries of Manipulator Workspaces. ASME Journal of Mechanical Design, 122(2000) 447-456.

[4] Gosselin C, Angeles J. The optimum kinematic design of a planar three-degree-of-freedom parallel manipulator. ASME Journal of mechanisms, Transmissions Automation in Design, 1988, 110(1): 35-41.

[5] Gosselin C, Angeles J. A global performance index for the kinematic optimization of robotic manipulators. ASME Journal of Mechanical Design, 1991, 113(3): 220-226.

[6] Xinhua Zhao, Wei Zhang. Parameter Optimization of the 3-RTT Parallel Manipulator Based on the Conditioning Index. China Mechanical Engineering, 2004, 15(21): 1903-1945.

[7] Toz M, Kucuk S. Dexterous workspace optimization of an asymmetric six-degree of freedom Stewart – Gough platform type manipulator. Robotics and Autonomous Systems, 61(2013) 1516-1528.

[8] Pu Zhang, Zhenqing Yao, Zhengchun Du. Global Performance Index System for Kinematic Optimization of Robotic Mechanism. ASME Journal of Mechanical Design, 136(2014) 1-11.

[9] Merlet J P. Jacobian, Manipulability, Condition Number, and Accuracy of Parallel Robots. ASME Journal of Mechanical Design, 128(2006) 199-206.

[10] Lee. Suklan. Dual Redundant Arm Configuration Optimization with Task-Oriented Dual Arm Manipulability. IEEE TRANSACTIONS ON ROBOTICS AND AUTOMATION, 1989, 5(1): 78-97.

[11] Shaofei Zhang, Di Zhao. Theory of Matrix Tutorial. Beijing: China Machine Press, 2010.

[12] Jingjun Yu, Xinjun Liu, Xilun Ding. Mathematical foundation of robot mechanism. Beijing: China Machine Press, 2009.

[13] Chao Wu, Xin-Jun Liu, Liping Wang. Optimal Design of Spherical 5R Parallel manipulators Considering the Motion/Force Transmissibility. ASME Journal of Mechanical Design, 132(2010) 031002.

[14] Jihong Lee, A Study on the Manipulability Measures for Robot Manipulators. Proceeding of international conference on Intelligent Robots and systems, Grenoble, Sep. 1997, pp. 1458-1465.

[15] Jin-Oh Kim, Pradeep K. Khosla. Dexterity Measures for Design and Control of Manipulators. IEEE/RSJ International Workshop on Intelligent Robots and Systems. Osaka, Japan, Nov 3-5, 1991.